OPEN ACCESS

Clinical science

CorvisST biomechanical indices in the diagnosis of corneal stromal and endothelial disorders: an artificial intelligence-based comparative study

Vincent Michel Borderie ,[1] Cristina Georgeon,[1] Nassim Louissi,[1] Benjamin Memmi,[1] Malika Hamrani,[1] Nacim Bouheraoua,[1] Anatole Chessel[2]

► Additional supplemental material is published online only. To view, please visit the journal online (https://doi.org/10.1136/bjo-2025-327855).

[1]Ophthalmology, Hôpital National des 15-20, Paris, France
[2]Laboratory for Optics and Biosciences, Palaiseau, France

Correspondence to
Professor Vincent Michel Borderie;
vincent.borderie@upmc.fr

Received 10 May 2025
Accepted 26 September 2025

ABSTRACT

Aims To analyse the value of the CorvisST indices in diagnosing corneal stromal and endothelial disorders (CSEDs).

Methods This institutional retrospective case–control study included 903 eyes with a CSED and 597 normal eyes (controls), assessed with CorvisST and MS39. Main outcome measures: CorvisST indices. The collected data were divided into a training set (70%) and a test set (30%). Artificial intelligence frameworks were used to distinguish each disorder from controls and to classify corneas into seven groups: keratoconus, high-risk corneas for keratoconus, laser corneal refractive surgery (LCRS), endothelial disorders, stromal opacities, glaucoma corneas and normal corneas.

Results Stress-strain index (SSI) significantly increased with age in the control group. Compared with controls matched for age/sex, keratoconus was associated with Corvis Biomechanical Index (CBI) >0.51 (area under the curve, 0.99), Ambrósio's relational thickness horizontal (ARTh) <425.5 (0.97), deflection amplitude at the time of the first applanation (SPA-A1) <96.3 (0.97) and Pachy<522.4 µm (0.91); high-risk corneas with a difference in CBI between fellow eyes (CBI SYM) >0.14 (0.98), (L2) <1.95 (0.83) and Pachy<549.7 µm (0.71); LCRS with ARTh<455.1 (0.93) and CBI>0.35 (0.83); corneal endothelial disorders with Pachy SYM>19.7 µm (0.83), Pachy>569.1 µm (0.82) and CBI SYM>0.14 (0.77); stromal opacities with SPA-A1 SYM>11.8 (0.92), ARTh<569.9 (0.89), SSI SYM>0.14 (0.89) and CBI>0.22 (0.86). A logistic regression function using all indices reached an area under the receiver operating characteristic curve of 0.81 for glaucoma diagnosis. The TabPFN model provided the best accuracy (88.7%) for diagnosing the seven corneal conditions. SSI, SPA-A1, CBI and Pachy correlated with keratoconus grade. Keratoplasty for keratoconus improved but failed to restore normal corneal biomechanics.

Conclusions CorvisST indices are relevant for diagnosing CESDs and distinguishing various disorders from each other.

WHAT IS ALREADY KNOWN ON THIS TOPIC

⇒ The CorvisST device is a useful tool for differentiating keratoconus and other corneal ectasias from normal corneas.

WHAT THIS STUDY ADDS

⇒ CorvisST indices are relevant for diagnosing and grading various corneal endothelial and stromal disorders and distinguishing them from each other using artificial intelligence.

HOW THIS STUDY MIGHT AFFECT RESEARCH, PRACTICE OR POLICY

⇒ CorvisST augmented with artificial intelligence should be included in the assessment of corneal disorders.

INTRODUCTION

The cornea exhibits viscoelastic behaviour, which is crucial for maintaining its curvature and subsequent refractive power despite changes in intraocular pressure and various external forces, such as eye rubbing or external shocks. Corneal biomechanical properties are closely related to the ultrastructure of the stroma, which consists of several hundred 1–3 µm-thick stacked lamellae composed of collagen fibrils that are aligned and regularly packed.[1] The corneal viscoelastic behaviour is explained by the rearrangement and sliding of stromal lamellae, as well as the stretching of stromal striae under stress.[2 3] Corneal stiffness depends on intraocular pressure and corneal thickness, as stiffness increases with both pressure and thickness.[4]

Corneal biomechanical behaviour can be assessed with various technologies, including strip extensometry, eye inflation, Brillouin microscopy, air-puff systems, ultrasound elastography, optical coherence elastography, enzymatic digestion, acoustic radiation force, atomic force microscopy and lateral electronic speckle pattern shearing interferometry.[5–9] In routine practice, only air-puff systems are currently widely available for clinical assessment of corneal biomechanical behaviour.[10] They provide a global evaluation of corneal biomechanics.

In the present study, we assessed the diagnostic value of the CorvisST indices in normal and diseased corneas, considering their ability to distinguish stromal and endothelial disorders from normal corneas and to differentiate various corneal conditions from each other.

To cite: Borderie VM, Georgeon C, Louissi N, *et al*. *Br J Ophthalmol* Epub ahead of print: [*please include* Day Month Year]. doi:10.1136/bjo-2025-327855

METHODS

Study design

This study was a retrospective comparative analysis of a consecutive series of patients conducted at a national tertiary centre, Hôpital National des 15–20, Paris, France. Patients were assessed between 2016 and 2024.

Patients with the following seven corneal stromal conditions were included: keratoconus, high-risk corneas for keratoconus development (keratoconus high-risk), laser refractive surgery, corneal endothelial disorders, stromal opacities, glaucoma and normal corneas.

All eyes were assessed with CorvisST (Oculus Optikgeräte GmbH, Wetzlar, Germany) and specular corneal topography combined with spectral domain-optical coherence tomography (SD-OCT) (MS39, CSO, Firenze, Italy). Each CorvisST examination consisted of three measurements for each eye. The inclusion criteria were a diagnosis confirmed by a senior cornea subspecialist (VMB), a CorvisST examination and an MS39 examination performed by an experienced orthoptist (CG).

Diagnosis criteria for the keratoconus group were the following: positive keratoconus diagnosis based on slit-lamp examination, specular topography and SD-OCT, either with a history of ocular surgery (including collagen cross-linking, intracorneal ring segment implantation and keratoplasty) or no history. Keratoconus staging was performed using the Amsler-Krumeich classification.[11] The three postoperative keratoconus subgroups (ie, cross-linking, ring segment, keratoplasty) featured the same preoperative diagnosis criteria as the keratoconus group. The keratoconus high-risk group included three corneal conditions: keratoconus fruste (corneas with normal clinical features, topography and SD-OCT, and keratoconus diagnosed in the fellow eye), keratoconus-suspect corneas (corneas with normal clinical features and abnormal or borderline MS39 classification), and corneas with a family history (mother, father or child) of keratoconus and normal clinical features, topography and SD-OCT. The MS39 device computes several keratoconus indices used for classification (online supplemental figure). Abnormal and borderline cases featured at least one abnormal index. The laser refractive surgery group included normal eyes treated with photorefractive keratectomy (PRK) for myopia or hyperopia, laser-assisted in situ keratomileusis (LASIK) for myopia, or small incision lenticule extraction (SMILE) for myopia, with a normal postoperative outcome and at least 3 months of follow-up after surgery. The four laser refractive surgery subgroups were not matched or comparable in terms of the amount of preoperative refractive error. The endothelial corneal disorder group included eyes with Fuchs dystrophy, polymorphous posterior corneal dystrophy or pseudophakic bullous keratopathy, as confirmed by slit-lamp examination and SD-OCT, either non-operated or after Descemet's Membrane Endothelial Keratoplasty. Cornea guttata severity was not routinely assessed because the presence of corneal oedema was the primary criterion used to indicate the need for transplantation in corneal endothelial disorders. To assess the severity of endothelial disorders, we used several metrics computed from the MS39 csv files (ie, vertex pachymetry and four paracentral (1–2 mm, 2–3 mm, 3–4 mm and 4–5 mm zones)/vertex pachymetry ratios; decreased ratios being associated with central oedema in Fuchs dystrophy). The glaucoma group consisted of eyes with confirmed primary open-angle glaucoma, as determined by visual field testing, SD-OCT assessment of the optic disc and retinal nerve fibre layer, elevated intraocular pressure and a normal cornea at slit-lamp and MS39 examination, either non-operated under medical treatment or following filtering surgery. The control group consisted of normal eyes that underwent a CorvisST assessment. The inclusion criteria were as follows: the absence of ocular symptoms and eye disease, no contact lens wear, no history of ocular surgery or trauma, normal slit-lamp examination, normal SD-OCT scans and maps and normal corneal topography.

The main outcome measures were the 16 CorvisST indices (ie, L1, first applanation length; L2, second applanation length; V1, corneal velocity at first applanation; V2, corneal velocity at second applanation; PD, peak distance; Radius, radius of curvature at the highest concavity; DA, deformation amplitude; Pachy, central corneal thickness; SSI, stress-strain index; IOPnc, uncorrected intraocular pressure; bIOP, biomechanically corrected intraocular pressure; DA ratio, ratio between the Deformation Amplitude (vertical displacement) at the corneal apex and the Deformation Amplitude at 2 mm nasal and temporal from the apex; IR, inverse of the radius of curvature during the concave phase of the deformation; ARTH, Ambrósio's relational thickness horizontal; SPA-A1, deflection amplitude at the time of the first applanation; and CBI, Corvis Biomechanical Index) and the absolute values of the differences between fellow eyes (labelled as index name+SYM).

Artificial intelligence and statistical analysis

For each patient, one examination was randomly selected and designated as the primary examination. Statistical analyses were performed using a software programme (Statistica V.6.1; StatSoft France, Maisons-Alfort, France). Machine learning and deep learning algorithms were written in Python.

We first analysed the primary examinations of the control group. The Spearman rank correlation coefficient was used to assess the correlation between Corvis indices and age, and the Mann-Whitney test was used to assess differences between male and female patients.

We then conducted a case–control study using primary examination data. For each primary exam in the diseased groups, one primary examination from the control group was selected based on age and sex matching. When no age- and sex-matched controls were available, the case was excluded from the analysis. The observations from the control and disease groups were randomly divided into a training set (70%) and a validation set (30%) using stratified sampling. The receiver operating characteristic (ROC) analysis was performed using data from both the control group and the analysed disease group, assessing the quantitative variable's ability to distinguish corneas with the given disorder from normal ones. The training set was used to determine the threshold value of the quantitative variable, and the validation set was used to calculate the area under the ROC curve (AUC) associated with the threshold value, sensitivity, specificity and accuracy (percentage of well-classified observations). CorvisST indices were considered relevant for diagnosing a given disorder when the AUC in the test set was greater than 0.50.

The subgroup analysis was performed using primary examinations. The CorvisST indices were analysed with analysis of variance and the appropriate post hoc tests. For the disorder diagnosis study, we trained 12 machine learning and deep learning classifiers using all examinations. Using stratified sampling, the data were randomly divided into a training set (70% of the examinations) and a test set (30% of the examinations). We performed hyperparameter tuning using grid search. The accuracy, that is, the percentage of well-classified observations, was assessed in the test set.

Table 1 Correlation between age and Corvis indices in normal corneas

	Age	V1	PD	DA	IOPnc	DA ratio	IR	SPA-A1
Age	**1.00**							
V1	0.06	**1.00**						
PD	**0.20**	**0.61**	**1.00**					
DA	**0.23**	**0.76**	**0.77**	**1.00**				
IOPnc	**−0.12**	**−0.77**	**−0.66**	**−0.77**	**1.00**			
DA ratio	**0.14**	**0.74**	**0.45**	**0.57**	**−0.68**	**1.00**		
IR	0.04	**0.70**	**0.39**	**0.56**	**−0.59**	**0.78**	**1.00**	
SPA-A1	0.08	**−0.76**	**−0.43**	**−0.57**	**0.67**	**−0.67**	**−0.61**	**1.00**

307 Corvis examinations from 307 randomly selected eyes of 307 patients are included in this correlation study. Shown is the Spearman correlation coefficient. Bold shows correlation coefficients with p<0.05. The absolute value of the difference between the fellow eyes is labelled as INDEX SYM. Only the most relevant indices are shown. Full data are shown in online supplemental table 1. DA, deformation amplitude; DA ratio, ratio between the deformation amplitude (vertical displacement) at the corneal apex and the deformation amplitude at 2 mm nasal and temporal from the apex; IOPnc, uncorrected intraocular pressure; IR, inverse of the radius of curvature during the concave phase of the deformation; PD, peak distance; SPA-A1, deflection amplitude at the time of the first applanation; V1, corneal velocity at first applanation.

RESULTS

A total of 1500 Corvis examinations from 772 patients (422 females and 350 males) were analysed. There were 427 examinations in the keratoconus group, 62 in the keratoconus high-risk group, 112 in the laser refractive surgery group, 168 in the endothelial disorder group, 45 in the stromal opacity group, 89 in the glaucoma group and 597 in the normal (control) group.

Control group

A total of 307 randomly selected normal corneas from 307 patients were analysed. Most CorvisST indices showed significant correlation with age (table 1, online supplemental table 1). SSI showed the strongest correlation (r_s=0.48) with age, increasing by an average of 0.07 units per decade (online supplemental figure). Most indices correlated with the central corneal thickness (Pachy). The CBI showed the strongest correlation (rs=−0.69) with Pachy, increasing with decreasing corneal thickness (on average, 0.03 units per 10 µm; online supplemental figure). All indices correlated with IOPnc; bIOP showed the strongest correlation (r_s=0.82). Finally, most indices significantly correlated with each other (table 1).

No significant differences were observed between males and females for all CorvisST indices, except for PD, SSI and ARTh, which were significantly higher (median, 4.91 vs 4.79, p=0.0006), lower (0.92 vs 0.98, p=0.03) and higher (600.9 vs 543.8, p=0.0004) in males, respectively, compared with females.

Case–control study

Study and matched control groups featured the same sex ratio and non-significantly different patient ages (online supplemental figure). Among 32 Corvis indices and absolute values of the differences between fellow eyes, the number of relevant indices was 30 for keratoconus diagnosis, 23 for keratoconus high-risk diagnosis, 12 for laser refractive surgery diagnosis, 16 for endothelial disorder diagnosis, 24 for stromal opacity diagnosis and 13 for glaucoma diagnosis. Table 2 presents the results of the case-control study for indices with an AUC of 0.70 or higher. Keratoconus was associated with CBI>0.51 (AUC, 0.99), ARTh<425.5 (0.97), SPA-A1<96.3 (0.97) and Pachy<522.4 µm (0.91). Keratoconus high-risk corneas were associated with a difference in CBI between fellow eyes (CBI SYM) >0.14 (0.98), L2<1.95 (0.83) and Pachy<549.7 µm (0.71). Laser refractive surgery was associated with ARTh<455.1 (0.93) and CBI>0.35 (0.83). Corneal endothelial disorders were associated with Pachy SYM>19.7 µm (0.83), Pachy>569.1 µm (0.82) and CBI SYM>0.14 (0.77). Corneas with stromal opacities were associated with SPA-A1 SYM>11.8 (0.92), ARTh<569.9 (0.89), SSI SYM>0.14 (0.89) and CBI>0.22 (0.86). A logistic regression function using all indices reached an AUC of 0.81 for glaucoma diagnosis.

Subgroup analysis

Keratoconus, whether untreated or after crosslinking, intracorneal ring segment implantation and keratoplasty, exhibited lower corneal stiffness, as assessed by SSI and SPA-A1, compared with normal corneas (post hoc tests, p<0.00003; figure 1). A higher Amsler-Krumeich grade was associated with lower stiffness and pachymetry, as well as higher CBI (p<0.01; figure 1). All keratoconus subgroups featured lower ARTh and higher CBI than normal corneas (p<0.01; figure 1). All keratoconus subgroups, except the keratoplasty subgroup (p=0.07), exhibited lower pachymetry compared with normal corneas (p<0.00001; figure 1). Post cross-linking and post-keratoplasty keratoconus corneas were significantly stiffer than keratoconus grade 3 and 4 but not than grade 1 and 2 (p<0.05). Keratoconus corneas with ring segments did not feature significantly greater SPA-A1 than non-operated keratoconus corneas (p>0.05). The three keratoconus high-risk subgroups exhibited significantly higher CBI and CBI SYM values compared with normal corneas (p<0.03; online supplemental figure). Keratoconus fruste corneas showed significantly higher CBI SYM values than keratoconus-suspect corneas and corneas with a family history of keratoconus (p<0.00005; online supplemental figure). The three myopic laser refractive surgery subgroups featured significantly higher CBI and lower ARTh than both the hyperopic PRK subgroup and the normal group (p<0.01; online supplemental figure). No significant differences were found between the three myopic laser refractive surgery subgroups (p>0.20). In the endothelial corneal disorder group, vertex pachymetry correlated with 11 indices, including Pachy (r_s=0.97, p=0.0001), DA ratio (r_s=−0.57, p=0.0001; online supplemental figure) and SPA-A1 (r_s=0.54, p=0.0001). In non-operated Fuchs dystrophy corneas, the paracentral/vertex pachymetry ratios correlated with Pachy (−0.78<r_s<−0.41, p=0.0001), SSI SYM (−0.69<r_s<−0.54, p=0.0001), CBI SYM (−0.53<r_s<−0.45, p<0.003), SSI (−0.53<r_s<−0.38, p<0.02), CBI (−0.50<r_s<−0.19, p<0.02) and ARTh (0.35<r_s<0.51, p<0.03). Keratoplasty in eyes with endothelial disorders was associated with lower Pachy (p<0.000001), higher Pachy SYM (p=0.005), lower ARTh (p=0.00004) and higher CBI (p<0.000001) compared with non-operated eyes. In the glaucoma group, filtering surgery was associated with a lower SPA-A1 (p=0.02) and higher asymmetry of most indices compared with non-operated eyes.

Disorder diagnosis with CorvisST indices

We first analysed the data, excluding eyes that underwent surgery in addition to the primary diagnosis. A total of 1268 CorvisST examinations were included in the analysis. The LightGBM model achieved the highest accuracy (86.9%) in the test set using CorvisST indices, symmetry indices and age (table 3). The confusion matrix in the test set is shown in table 4. Online supplemental figure shows the parameter importances in the

Table 2 Case–control study

Groups	Corvis index	Study group: mean±SD (train set)	Control group: mean±SD (train set)	Threshold value (train set)	AUC (test set)	Se (%) (test set)	Sp (%) (test set)	Ac (%) (test set)
Keratoconus vs control (n=370)	CBI	0.86+0.22	0.19+0.19	0.51	0.99	94.5	91.1	92.8
	ARTh	240.5+145.6	574.2+124.1	425.5	0.97	83.6	98.2	91.0
	SPA-A1	74.1+22.7	116.1+18.9	96.3	0.97	83.6	100.0	91.9
	All parameters				0.96	89.6	96.8	93.7
	IR	12.8+3.7	8.6+1.3	9.9	0.95	85.5	92.9	89.2
	Radius	5.14+1.06	6.78+0.84	6.08	0.94	90.9	85.7	88.3
	DA ratio	5.87+1.71	4.21+0.46	4.69	0.91	87.3	87.5	87.4
	Pachy	475.7+64.6	556.2+35.8	522.4	0.91	78.2	96.4	87.4
	Pachy SYM	40.8+50.4	9.4+7.6	16.1	0.88	92.7	73.2	82.9
	DA	1.23+0.17	1.06+0.1	1.13	0.88	80.0	89.3	84.7
	IOPnc	14.1+2.6	17.4+2.6	15.8	0.86	81.8	76.8	79.3
	IR SYM	2.48+2.83	0.57+0.92	0.99	0.85	90.9	62.5	76.6
	DA ratio SYM	1.10+1.26	0.18+0.17	0.35	0.84	83.6	75.0	79.3
	SSI	0.74+0.19	0.92+0.18	0.83	0.83	80.0	78.6	79.3
	V1	0.18+0.03	0.15+0.02	0.16	0.82	61.8	96.4	79.3
	V2	−0.41+1.02	−0.27+0.03	−0.29	0.81	81.8	64.3	73.0
	L2	1.51+0.4	1.95+0.38	1.73	0.80	81.8	73.2	77.5
	L1	1.91+0.35	2.17+0.37	2.04	0.75	90.9	42.9	66.7
	DA SYM	0.11+0.09	0.06+0.04	0.07	0.74	81.8	58.9	70.3
	V1 SYM	0.02+0.02	0.01+0.01	0.02	0.73	90.9	39.3	64.9
	V2 SYM	0.04+0.04	0.02+0.02	0.03	0.73	98.2	21.4	59.5
	SPA-A1 SYM	17.8+12.6	13.1+32.9	14.0	0.71	72.7	69.6	71.2
Keratoconus high-risk vs control (n=64)	CBI SYM	0.28+0.23	0.08+0.07	0.14	0.98	100.0	90.0	95.0
	L2	1.87+0.25	2.05+0.50	1.95	0.83	90.0	60.0	75.0
	V1 SYM	0.02+0.01	0.01+0.01	0.01	0.77	70.0	80.0	75.0
	SSI SYM	0.08+0.09	0.06+0.04	0.07	0.75	100.0	30.0	65.0
	SPA-A1 SYM	14.0+14.8	12.7+10.4	13.3	0.74	80.0	60.0	70.0
	CBI	0.36+0.27	0.11+0.12	0.20	0.71	90.0	60.0	75.0
	Radius SYM	0.65+0.56	0.50+0.30	0.57	0.71	90.0	60.0	75.0
	L2 SYM	0.36+0.23	0.41+0.28	0.38	0.71	90.0	40.0	65.0
	Pachy	534.1+31.6	566.4+38.8	549.7	0.71	90.0	60.0	75.0
	L1 SYM	0.31+0.25	0.42+0.25	0.36	0.71	80.0	60.0	70.0
Laser refractive surgery vs control (n=104)	ARTh	334.0+187.5	570.2+122.8	455.1	0.93	92.3	100.0	96.3
	CBI	0.53+0.38	0.23+0.23	0.35	0.83	92.3	57.1	74.1
	All parameters				0.79	83.3	66.7	74.1
	Radius	6.33+0.99	6.84+0.62	6.61	0.73	92.3	50.0	70.4
Endothelial disorder vs control (n=166)	All parameters				0.87	70.0	96.7	86.0
	Pachy SYM	64.7+56.3	11.0+6.7	19.7	0.83	72.0	96.0	84.0
	Pachy	589.1+54.6	550.8+36.4	569.1	0.82	76.0	92.0	84.0
	CBI SYM	0.22+0.23	0.09+0.11	0.14	0.77	100.0	24.0	62.0
	V1	0.14+0.02	0.14+0.02	0.14	0.74	96.0	32.0	64.0
Stromal opacity vs control (n=52)	SPA-A1 SYM	18.0+16.0	8.5+6.5	11.8	0.92	100.0	62.5	81.2
	ARTh	524.3+337.8	618.3+202.2	569.9	0.89	87.5	100.0	93.8
	SSI SYM	0.19+0.21	0.11+0.09	0.14	0.89	100.0	62.5	81.2
	CBI	0.34+0.31	0.14+0.14	0.22	0.86	75.0	100.0	87.5
	CBI SYM	0.07+0.11	0.05+0.05	0.06	0.83	100.0	75.0	87.5
	IOPnct SYM	3.6+4.2	1.2+0.9	1.9	0.81	87.5	50.0	68.8
	Pachy	540.7+72.7	557.1+34.4	549.3	0.77	87.5	62.5	75.0
	Pachy SYM	42.9+59.4	9.4+8.1	16.8	0.73	87.5	62.5	75.0
	PD SYM	0.21+0.2	0.13+0.12	0.17	0.73	87.5	62.5	75.0
	bIOP	16.9+2.9	15.5+1.9	16.2	0.73	75.0	62.5	68.8
	SPA-A1	109.2+28.4	122.2+13.4	116.1	0.72	100.0	37.5	68.8
	DA ratio SYM	0.37+0.49	0.09+0.10	0.16	0.71	75.0	62.5	68.8
	Radius	7.01+1.37	7.15+0.63	7.08	0.70	87.5	75.0	81.2
Glaucoma vs control (n=102)	All parameters				0.81	93.8	53.3	74.2

Only indices with an area under the receiver operating characteristic curve of at least 0.70 in the test set are shown.
Ac, accuracy; ARTH, Ambrósio's relational thickness horizontal; AUC, the area under the receiver operating characteristic curve; bIOP, biomechanically corrected intraocular pressure; CBI, Corvis Biomechanical Index; DA ratio, ratio between the deformation amplitude (vertical displacement) at the corneal apex and the deformation amplitude at 2 mm nasal and temporal from the apex; IOPnc, uncorrected intraocular pressure; L1, first applanation length; L2, second applanation length; PD, peak distance; Radius, radius of curvature at the highest concavity; Se, sensitivity; Sp, specificity; SPA-A1, deflection amplitude at the time of the first applanation; SSI, stress-strain index; SYM, the absolute value of the difference between fellow eyes (eg, CBI SYM is the absolute value of the difference in CBI between fellow eyes); V1, corneal velocity at first applanation; V2, corneal velocity at second applanation.

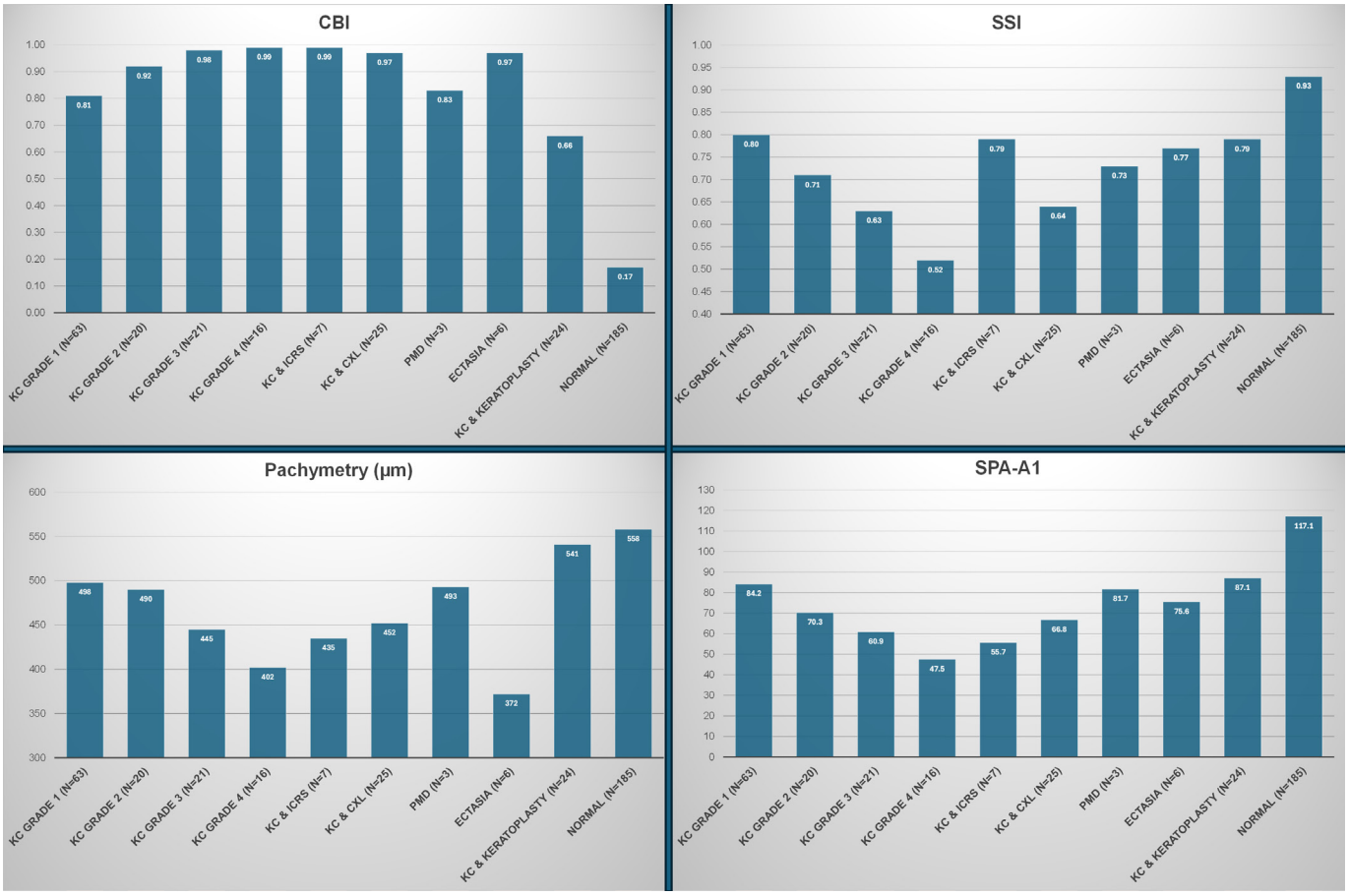

Figure 1 Corvis indices in the keratoconus subgroups. Analysis of variance: p<0.000001 for the four indices. CBI, Corvis Biomechanical Index; CXL, cross-linking; ICRS, intracorneal ring segment; KC, keratoconus; PMD, pellucid marginal degeneration; SPA- A1, deflection amplitude at the time of the first applanation; SSI, stress-strain index.

LightGBM model. We then analysed data, including eyes with surgery in addition to the primary diagnosis. A total of 1500 Corvis examinations were included in the analysis. The TabPFN deep learning model featured the highest accuracy (88.7%) (tables 3 and 4).

Table 3 Accuracy of the various trained artificial intelligence models

Model	Accuracy (test set)	
	Primary diagnosis with no additional surgery (n=1268) (%)	Primary diagnosis, with or without additional surgery (n=1500) (%)
TabPFN	86.1	88.7
LightGBM	86.9	86.4
XGBoost	86.1	84.0
Gradient Boosting	84.3	84.2
CatBoost	83.5	83.8
Random Forest	82.2	82.2
SVM	75.3	69.3
Decision Tree	75.1	71.6
MLP Classifier	74.8	59.1
Logistic Regression	71.1	71.8
KNN	70.9	68.4
Naive Bayes	64.6	63.1

DISCUSSION

From the case–control study, we identified some findings that are helpful for physicians in diagnosing stromal and endothelial corneal disorders. Keratoconus corneas were softer and thinner, and they featured increased CBI compared with normal ones. In a previous study, we reported significant differences between keratoconus and normal corneas for all CorvisST indices, even after adjustment for pachymetry and intraocular pressure.[12] CorvisST measurements in keratoconic and normal eyes are highly repeatable and reproducible.[13] Keratoconus high-risk corneas were softer and thinner with asymmetric CBI compared with normal corneas. They could be differentiated from normal corneas with a 0.98-AUC. Interestingly, all keratoconus high-risk subgroups, including patients with a family history of keratoconus and normal topography and tomography, featured the same biomechanical characteristics. For the detection of forme fruste keratoconus, CBI sensitivity was reported to be 63.2% with a specificity of 80.3%.[14] Its diagnostic ability is comparable to that of the Pentacam indices for differentiating normal eyes and eyes with forme fruste keratoconus.[14] In a recent study, a logistic regression model using both Pentacam and Corvis data reached an AUC of 0.90 for differentiating suspected from subclinical keratoconus.[15] TBI (Tomographic and Biomechanical Index) optimised for ethnicity can distinguish normal from early ectasia corneas with an AUC of 0.93.[16]

Laser refractive surgery corneas were thinner with increased CBI compared with normal ones. Following PRK, LASIK and

Table 4 Confusion matrices in the test set: LightGBM model trained on eyes with no surgery in addition to the primary diagnosis, and TabPFN model trained on eyes with or without surgery in addition to the primary diagnosis

Confusion matrices in the test set									
		Predicted							
LightGBM model, only primary diagnosis									
		Refractive surgery	Glaucoma	Keratoconus high risk	Keratoconus	Normal	Oedema	Stromal opacity	
True	Refractive surgery	**27**	0	0	3	3	0	1	*34*
	Glaucoma	0	**7**	0	0	9	1	0	*17*
	Keratoconus high risk	0	1	**11**	2	3	1	0	*18*
	Keratoconus	3	0	2	**86**	1	0	1	*93*
	Normal	0	3	0	0	**172**	4	0	*179*
	Oedema	0	3	0	2	1	**22**	0	*28*
	Stromal opacity	0	0	0	1	5	0	**6**	*12*
		30	*14*	*13*	*94*	*194*	*28*	*8*	*381*
TabPFN model, primary diagnosis, with or without subsequent surgery									
True	Refractive surgery	**27**	2	0	1	3	0	1	*34*
	Glaucoma	0	**12**	0	1	13	1	0	*27*
	Keratoconus high risk	0	1	**11**	2	3	2	0	*19*
	Keratoconus	0	2	0	**124**	1	0	1	*128*
	Normal	1	1	0	0	**173**	4	0	*179*
	Oedema	0	1	0	1	1	**47**	0	*50*
	Stromal opacity	0	1	0	2	3	2	**5**	*13*
		28	*20*	*11*	*131*	*197*	*56*	*7*	*450*

Bold corresponds to correctly classified cases

SMILE, significant changes in CorvisST indices have been demonstrated, including a decrease in bIOP, ARTH and SP-A1, together with an increase in DA ratio, IR and CBI. As expected, we found that myopic treatment induced more changes in corneal biomechanical behaviour compared with hyperopic treatment. We found no significant differences among the three myopic subgroups; however, the amount of preoperative myopia was not comparable. Previous studies found the decrease in corneal stiffness to be lower after PRK than SMILE, and lower after SMILE than after LASIK.[17–19] In eyes with a history of laser refractive surgery, CBI-LVC enables the accurate diagnosis of postoperative ectasia.[20]

Corneal endothelial disorders were characterised by increased and asymmetric central corneal thickness, as well as asymmetric CBI. As expected, they were thicker with an increased difference between fellow eyes and featured increased bIOP. They were neither stiffer nor softer than normal ones. However, increased corneal oedema was associated with increased stiffness. In non-operated Fuchs dystrophy corneas, increased central oedema (decreased paracentral/vertex ratios) was associated with increased stiffness, CBI and index asymmetry. A longer L1 has been reported to be associated with the advanced stage of Fuchs' dystrophy.[21] In healthy young adults, SPA-A1 increases with corneal thickness during diurnal variations of stromal hydration.[22]

Corneas with stromal opacity were characterised by asymmetric corneal stiffness, decreased central corneal thickness and increased CBI.

Glaucoma was associated with increased differences between fellow eyes in several indices. However, only a logistic regression function using all indices could achieve an AUC greater than 0.70, indicating that no single, simple biomechanical feature can characterise glaucoma corneas.

Although these features are insufficient for diagnosing the disorders, they may help make a decision when clinical findings, topography and tomography reveal other characteristics of a disorder. Interestingly, the indices and differences between fellow eyes were relevant for diagnosing the disorders. Loss of symmetry and enantiomorphism is a well-known characteristic of keratoconus. We demonstrate here that keratoconus high-risk corneas, corneas undergoing laser refractive surgery, corneal endothelial disorders, corneas with stromal opacity and glaucoma eyes exhibit non-symmetrical corneal biomechanical behaviour.

CorvisST data provides a wealth of information that clinicians may find challenging to handle fully. Many indices depend on the patient's age, corneal thickness and intraocular pressure. Whereas a trained clinician would easily suspect keratoconus on CorvisST examinations with no additional information, they would have difficulty suspecting the other disorders included in the present study. Conversely, artificial intelligence algorithms applied to CorvisST examinations could diagnose various disorders with a high accuracy of nearly 90%, meaning that only 1 out of 10 diagnoses was incorrect. A technician can perform Corvis as a quick exam, making it suitable for use as a screening tool or as part of a comprehensive workup that includes topography and SD-OCT.

The subgroup analysis provided valuable insights into several disorders. SSI, SPA-A1, CBI and Pachy correlated with keratoconus grade, showing they all were indicative of disease severity. A Corvis-derived parameter 'E' provides a biomechanical staging for ectasia and keratoconus. The linear term of the CBI is highly associated with keratoconus severity as defined by corneal tomography.[23]

As expected, keratoconus corneas were softer than normal ones. However, none of the keratoconus surgical procedures, including keratoplasty, ring segment implantation and cross-linking (although tending to improve), can restore normal corneal biomechanical behaviour, indicating that the ideal treatment for keratoconus remains to be discovered. Although studies have demonstrated an increase in corneal stiffness, many CorvisST indices remain unchanged after

cross-linking.[24 25] Keratoconus fruste corneas, keratoconus suspect corneas and corneas with a family history of keratoconus exhibit significantly higher CBI and a greater difference in CBI between fellow eyes compared with normal ones. These indicators are relevant for screening candidates for refractive surgery who exhibit a significantly increased prevalence of keratoconus.[26]

The study's limitations include its retrospective and monocentric design. The AI algorithms that were trained only apply to our study population. If they were to be used in another centre, a local dataset would be needed to fit the models. However, the method for reaching efficient models can be easily reproduced in other centres, given the methodology described here.

In conclusion, CorvisST indices are relevant for diagnosing corneal stromal and endothelial disorders and for distinguishing various disorders from one another. Analysis of key indices provides the physician with pertinent information to consider together with clinical, tomographic and topographic data. Artificial intelligence enables the consideration of all indices, including complex non-linear relationships, thereby improving diagnosis accuracy.

Contributors Guarantor: VMB; design of the study: VMB; conduct of the study: VMB, CG, NL, AC; collection, management, analysis and interpretation of data: VMB, CG, NL, BM, MH, NB, AC; preparation, review and approval of manuscript: VMB, CG, NL, BM, MH, NB, AC.

Funding Supported by the Agence Nationale de la Recherche (grant # ANR-21-CE19-0010-02, CorMecha project). The sponsor or funding organisation had no role in the design, conduct or reporting of this research. The authors have no financial or proprietary interest in any material or method mentioned in the paper.

Competing interests None declared.

Patient consent for publication Not applicable.

Ethics approval This study involves human participants and was approved by the Ethics Committee of the French Society of Ophthalmology (IRB 00008855 Société Française d'Ophtalmologie IRB#1). It followed the tenets of the Declaration of Helsinki and informed consent approval. Participants gave informed consent to participate in the study before taking part.

Provenance and peer review Not commissioned; externally peer reviewed.

Data availability statement Data are available upon reasonable request.

ORCID iD

Vincent Michel Borderie https://orcid.org/0000-0002-1395-8483

REFERENCES

1 Tidu A, Schanne-Klein MC, Borderie VM. Development, structure, and bioengineering of the human corneal stroma: A review of collagen-based implants. *Exp Eye Res* 2020;200:108256.
2 Grieve K, Ghoubay D, Georgeon C, *et al*. Stromal striae: a new insight into corneal physiology and mechanics. *Sci Rep* 2017;7:13584.
3 Wu Q, Giraudet C, Allain JM. Mechanical properties of stromal striae, and their impact on corneal tissue behavior. *J Mech Behav Biomed Mater* 2024;160:106770.
4 Roberts CJ. Importance of accurately assessing biomechanics of the cornea. *Curr Opin Ophthalmol* 2016;27:285–91.
5 Kling S, Hafezi F. Corneal biomechanics - a review. *Ophthalmic Physiol Opt* 2017;37:240–52.
6 Singh M, Li J, Vantipalli S, *et al*. Noncontact Elastic Wave Imaging Optical Coherence Elastography for Evaluating Changes in Corneal Elasticity Due to Crosslinking. *IEEE J Sel Top Quantum Electron* 2016;22:6801911.
7 Wilson A, Marshall J, Tyrer JR. The role of light in measuring ocular biomechanics. *Eye (Lond)* 2016;30:234–40.
8 Piñero DP, Alcón N. Corneal biomechanics: a review. *Clin Exp Optom* 2015;98:107–16.
9 Li J, Han Z, Singh M, *et al*. Differentiating untreated and cross-linked porcine corneas of the same measured stiffness with optical coherence elastography. *J Biomed Opt* 2014;19:110502.
10 Piñero DP, Alcón N. In vivo characterization of corneal biomechanics. *J Cataract Refract Surg* 2014;40:870–87.
11 Baenninger PB, Bodmer NS, Bachmann LM, *et al*. Keratoconus Characteristics Used in Randomized Trials of Surgical Interventions-A Systematic Review. *Cornea* 2020;39:615–20.
12 Borderie V, Beauruel J, Cuyaubère R, *et al*. Comprehensive Assessment of Corvis ST Biomechanical Indices in Normal and Keratoconus Corneas with Reference to Corneal Enantiomorphism. *J Clin Med* 2023;12:690.
13 Yang K, Xu L, Fan Q, *et al*. Repeatability and comparison of new Corvis ST parameters in normal and keratoconus eyes. *Sci Rep* 2019;9:15379.
14 Wang YM, Chan TCY, Yu M, *et al*. Comparison of Corneal Dynamic and Tomographic Analysis in Normal, Forme Fruste Keratoconic, and Keratoconic Eyes. *J Refract Surg* 2017;33:632–8.
15 Peng Y, Feng Q, Shao T, *et al*. Differences between suspected keratoconus and subclinical keratoconus via multiparameter analysis in Chinese populations. *Sci Rep* 2025;15.
16 Huo Y, Xie R, Li J, *et al*. Ethnicity optimized indices enhance the diagnostic efficiency of early Keratoconus: A multicenter validation study. *Cont Lens Anterior Eye* 2025;48:102382.
17 Abd El-Fattah EA, El Dorghamy AA, Ghoneim AM, *et al*. Comparison of corneal biomechanical changes after LASIK and F-SMILE with CorVis ST. *Eur J Ophthalmol* 2021;31:1762–70.
18 Joshi S, Bari A, Shakkarwal C, *et al*. The visual outcomes and corneal biomechanical properties after PRK and SMILE in low to moderate myopia. *Indian J Ophthalmol* 2025;73:128–33.
19 Qu Z, Li X, Yuan Y, *et al*. In Vivo Corneal Biomechanical Response to Three Different Laser Corneal Refractive Surgeries. *J Refract Surg* 2024;40:e344–52.
20 Vinciguerra R, Ambrósio R Jr, Elsheikh A, *et al*. Detection of postlaser vision correction ectasia with a new combined biomechanical index. *J Cataract Refract Surg* 2021;47:1314–8.
21 Reinprayoon U, Jermjutitham M, Kasetsuwan N. Rate of Cornea Endothelial Cell Loss and Biomechanical Properties in Fuchs' Endothelial Corneal Dystrophy. *Front Med (Lausanne)* 2021;8:757959.
22 Zhu D, Wang L, Qu Z, *et al*. Diurnal variations in corneal biomechanics in healthy young adults. *BMC Ophthalmol* 2025;25:90.
23 Flockerzi E, Vinciguerra R, Belin MW, *et al*. Correlation of the Corvis Biomechanical Factor with tomographic parameters in keratoconus. *J Cataract Refract Surg* 2022;48:215–21.
24 Herber R, Francis M, Spoerl E, *et al*. Evaluation of Biomechanical Changes After Accelerated Cross-Linking in Progressive Keratoconus: A Prospective Follow-Up Study. *Cornea* 2023;42:1365–76.
25 Felter E, Khoramnia R, Friedrich M, *et al*. Biomechanical changes following corneal crosslinking in keratoconus patients. *Graefes Arch Clin Exp Ophthalmol* 2024;262:3635–42.
26 Randleman JB, Russell B, Ward MA, *et al*. Risk factors and prognosis for corneal ectasia after LASIK. *Ophthalmology* 2003;110:267–75.